molecules

MDPI

Article

Chemical Constituent Profiling of *Paecilomyces cicadae* Liquid Fermentation for *Astragli Radix*

Yuqi Wang [1], Xiaodan Mei [1], Zihan Liu[1], Jie Li [1], Xiaoxin Zhang [1], Shaoping Wang [2], Zikai Geng [2], Long Dai [2,*] and Jiayu Zhang[1,2,*]

[1] School of Chinese Pharmacy, Beijing University of Chinese Medicine, Beijing 100029, China
[2] School of Pharmacy, BIN ZHOU Medical University, Yantai 260040, China
* Correspondence: druglab@sina.com (L.D.); zhangjiayu0615@163.com (J.Z.);
Tel: +86-10-0535-6913719 (L.D.); Tel: +86-10-0535-6913719 (J.Z.)

Received: 1 August 2019; Accepted: 12 August 2019; Published: 14 August 2019

Abstract: *Astragli Radix* (AR) is one of the most popular traditional Chinese medicines with chemical constituents including flavonoids and saponins. As recently evidenced, some fungi or their fermentation liquid may have the potential to affect the bioactive constituents and different pharmacological effects of AR. Thus, the composition of fermented AR (FAR) produced by *Paecilomyces cicadae* (Miquel) Samson in liquid-state fermentation was investigated using a UHPLC-LTQ-Orbitrap mass spectrometer in both positive and negative ion modes. Firstly, the MS^n data sets were obtained based on a data-dependent acquisition method and a full scan–parent ions list–dynamic exclusion (FS-PIL-DE) strategy. Then, diagnostic product ions (DPIs) and neutral loss fragments (NLFs) were proposed for better constituent detection and structural characterization. Consequently, 107 constituents in total, particularly microconstituents in FAR and AR, were characterized and compared in parallel on the same LTQ–Orbitrap instrument. Our results indicated that AR fermentation with *Paecilomyces* significantly influenced the production of saponins and flavonoids, especially increasing the content of astragaloside IV. In conclusion, this research was not only the first to show changes in the chemical components of unfermented AR and FAR, but it also provides a foundation for further studies on the chemical interaction between microbiota and AR.

Keywords: Astragli Radix; *Paecilomyces cicadae;* liquid fermentation; chemical constituents; UHPLC-LTQ-Orbitrap MS.

1. Introduction

Over the past several decades, accompanied by growing demand for traditional Chinese medicines (TCMs) and a gradual reduction of wild resources, improving the content of active ingredients and cultivating new varieties with high quality have become the most urgent tasks in the development of herbal resources. Recently, the application of TCMs by submerged fermentation of edible and pharmaceutical fungi has become a hot issue which opens up broad prospects for TCMs. Previous studies have shown that medicinal fungi can secrete important secondary metabolic products which degrade macromolecular material into small molecules [1,2]. By means of fermentation, TCMs can improve intrinsic conversion efficiency and new compound growth rates for increased therapeutic effect. Besides this, fermentation can also reduce the toxicity of TCMs containing typical compounds such as alkaloids, lactones, toxic glycosides, toxic proteins, anthraquinones, tannins, and heavy metals [3,4].

Paecilomyces cicadae (Miquel) Samson, as an entomogenous and medicinal fungus, is thought to be the anamorph stage of *Cordyceps cicadae* Shing. It is widely used as a tonic for nourishment as well as a functional food, and it has attracted considerable attention due to its wide range of nutritional and pharmacological activities, including immunomodulatory [5], antioxidation, anti-aging, anti-tumor [6], and anti-inflammation activity and ameliorating renal function [7].

Astragli Radix (AR), known as Huangqi in Chinese, is one of the most widely used traditional herbal medicines. It is the dried root of *Astragalus membranaceus* (Fisch.) Bge. var. *mongholicus* (Bge.) Hsiao or *Astragalus membranaceus* (Fisch.) Bge. AR contains relatively high quantities of saponins, flavonoids, polysaccharides, and some trace elements, which are known for their antibacterial, anti-inflammatory, analgesic, anti-cancer, anti-oxidant, and other pharmacological effects [8–11]. However, different processing methods (such as fermentation) may change the properties of this material.

Many studies have reported that natural macromolecular compounds exist in herbal medicines, including polysaccharides, flavonoid glycosides, and saponins, which promote pharmacological anti-tumor, anti-oxidant, and anti-inflammatory effects. However, most herbal macromolecular compounds cannot be digested and used by the human being in the absence of microbial fermentation [12]. For example, polysaccharides fermented by microbiota can be converted into short-chain fatty acids, which are easily digested and absorbed by the human body [13]. In addition, when red ginseng is fermented by *Bifidobacterium* H-1, Rg3 is transformed to Rh2, which has exhibited potent cytotoxicity against tumor cells [14]. Therefore, the aim of our present study was to develop liquid-state fermentation for AR by *Paecilomyces cicadae* (Miquel) Samson and to investigate whether this method leads to changes in the components contained in AR.

In order to obtain comprehensive knowledge of the compounds in the fermented AR (FAR), we further characterized its chemical constituents by way of ultra-high-performance liquid chromatography coupled with high-resolution mass spectrometry (UHPLC-HRMS). Moreover, the application of a full scan–parent ions list–dynamic exclusion (FS-PIL-DE) strategy coupled with diagnostic product ions (DPIs) and neutral loss fragments (NLFs) is proposed for better constituent detection and structural characterization [15,16]. Finally, the constituents, particularly microconstituents in FAR and AR, were characterized and compared in parallel on the same LTQ-Orbitrap instrument.

2. Results

2.1. Establishment of the Analytical Strategy

In this study, a comprehensive and effective strategy is proposed to systematically screen and identify compounds on a UHPLC-LTQ-Orbitrap MS instrument. The analytic strategy roughly consisted of three steps. The first step was online data acquisition. A full mass scan was performed with a resolution of 30,000. Meanwhile, high-resolution extracted ion chromatography (HREIC) was adopted to extract the candidates from the high-quality, accurate raw mass data both in negative and positive ion modes. Secondly, PIL-DE and data-dependent acquisition methods were employed to obtain specific ESI-MS/MS datasets based on those screened candidates. Then, DPI and NLF techniques were used as supplementary tools for the selective detection of constituents that possess similar mass fragmentation behaviors to those of reference standards. Finally, the structures of the compounds were elucidated according to the accurate mass measurement, fragmentation patterns, diagnostic product ions, and literature reports. The general procedures of our strategy and approach are summarized in the diagram shown in Figure 1.

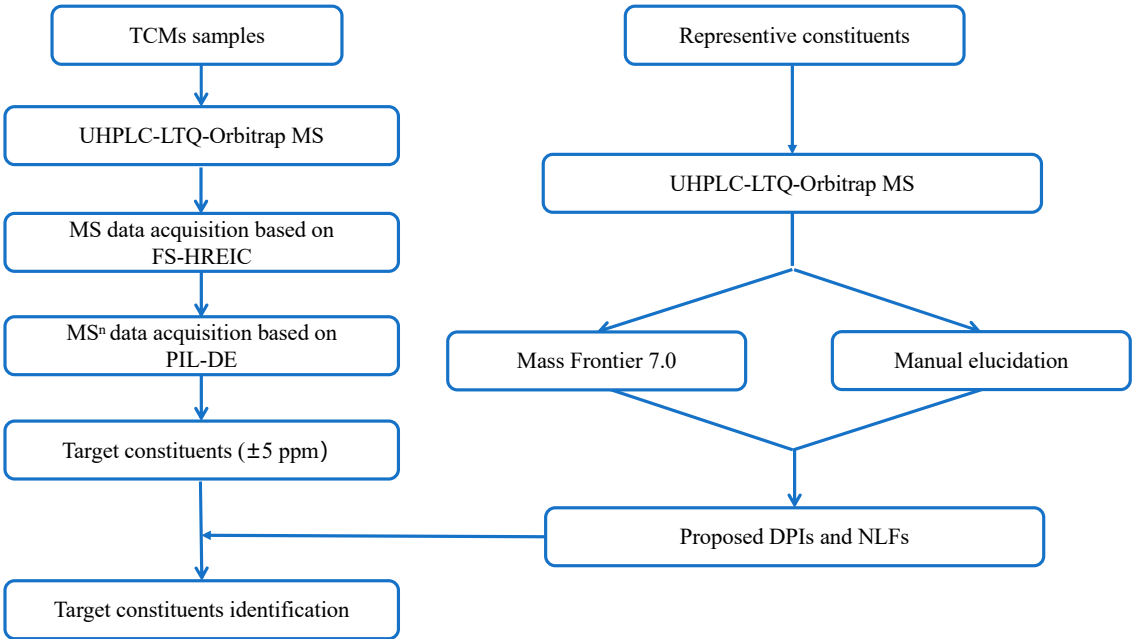

Figure 1. Summary diagram of the presently developed strategy and methodology.

2.2. Establishment of the Data Acquisition Methods

By employing the full scan method, abundant data were generated with large amounts of invalid data. Thus, to reduce potential disturbances by irrelevant substances and avoid missing target drug compounds (especially trace compounds), HREIC was developed for compound detection [17]. The application of HREIC could intelligently filter the background and matrix-related ions from drug-related ions according to the accurate mass of $[M-H]^-$ or $[M+H]^+$ ions. The molecular weights and elemental compositions of compounds derived from the accurate mass measurements can also be readily predicted. As a result, the lower level of target compounds can be captured clearly. For a complicated system, FS was not an appropriate approach to obtain the entire MS/MS dataset due to the numerous potential candidates. Therefore, the PIL-DE method served as a supplementary method to obtain the MS/MS fragmentation of the microconstituents [15]. By means of the PIL-DE method, MS/MS acquisition of predictable constituents that have the same molecular weights could be triggered due to its superior sensitivity and selectivity.

2.3. Fragmentation Pattern Analysis and DPI Determination

To facilitate the structural elucidation of constituents in AR and FAR, sixteen standards, including eight astragalus saponins and eight flavonoids, were subsequently analyzed by UHPLC-LTQ-Orbitrap MS. All the standards exhibited $[M-H]^-$ or $[M+H]^+$ ions of sufficient intensity that could be isolated automatically and subjected to collision induced dissociation (CID)-MS/MS analysis. Mass Frontier v7.0 software (Thermo Scientific, Waltham, MA, USA) and manual elucidation were used to acquire comprehensive structural identification of these reference compounds.

In CID mode, compounds are often divided into two parts, such as product ions (emerge in ESI-MS/MS spectra due to their property of being easily ionized) and neutral fragments (observed in ESI-MS/MS spectra due to their mass difference and neutral characteristics) [18,19], which are complementary in structure. It is well documented that compounds with similar backbone structure exhibit comparable fragmentation patterns, resulting in certain diagnostic product ions (DPIs) and regular neutral loss fragments (NLFs). Consequently, the combination of DPIs and NLFs was helpful to rapidly performing the structural elucidation [20,21].

Eight astragalus saponin standards were subsequently analyzed firstly in the CID-MS/MS experiment. For instance, astragaloside I, isoastragaloside I, astragaloside II, isoastragaloside II, and astragaloside IV possess the same backbone structure, and their differences are limited to the quantity and position of acetyl groups connected to xylose. For instance, there are two acetyl groups on the 2 and 3 positions of xylose in astragaloside I, one acetyl group on the 2 position of xylose in astragaloside II, and zero acetyl groups in astragaloside IV. By comparing the MS/MS spectra of their product ions, some characteristic dissociation pathways of astragalus saponins could be summarized, which provided a basis for further characterization of the other candidates. Taking the negative ion mode as an example, all of the deprotonated ions could lose one glucosyl ($C_6H_{10}O_5$·) or xylose ($C_5H_8O_4$·) or even both of them in their ESI-MS spectra. Then, the base peak ions of $[M-H-162]^-$, $[M-H-132]^-$, and $[M-H-294]^-$ could be formed. Owing to the special structure of the acetyl group (Ac), other characteristic fragment ions were also generated by the loss of 42 (Ac), 60 (Ac+H_2O), and 84 (2Ac). These diagnostic product ions could be employed to ascertain the structural skeletons of astragalus saponins and simplify the following structural elucidation.

In addition, we also selected eight flavonoids as subjects to determine their DPIs. Owing to the special structures of flavonoid glycosides, the base peak ion of $[M-H-162]^-$ was usually produced via the loss of the glucose moiety in their ESI-MS^2 spectra. Meanwhile, the other characteristic ions at $[M-H-15]^-$, $[M-H-18]^-$, $[M-H-28]^-$, $[M-H-29]^-$, $[M-H-31]^-$, $[M-H-43]^-$, $[M-H-44]^-$, and $[M-H-61]^-$ were yielded by losing CH_3, H_2O, CO, HCO, OCH_3, CH_3+CO, HCO + CH_3, and H_2O+CO+CH_3 in negative mode. Therefore, the DPIs mentioned above could be utilized for deducing the structures of related compounds from abundant complex constituents.

2.4. Structural Assignment of Chemical Constituents in AR and FAR

Saponins and flavonoids are the major chemical constituents in AR. As a result, 107 compounds in total were detected and characterized from AR and FAR by way of UHPLC-LTQ-Orbitrap MS with the established strategy. Among these compounds, 42 were attributed to saponins while the remaining 65 were identified as flavonoids. The correlative data are summarized in Tables 1 and 2, and the HREIC spectra of detected constituents are illustrated in Figure 2. The fragmentation patterns of representative saponins and flavonoids are shown in Figures S1 and S2.

Table 1. Summary of identified saponins in Astragli Radix (AR) and fermented AR (FAR).

Peak	t_R /min	Ion Mode	Formula	Theoretical Mass *m*/*z*	Experimental Mass *m*/*z*	Error (ppm)	MS^2/MS^3 Fragment Ions	Identification	FAR	AR
A1	7.57	P	$C_{48}H_{79}O_{18}$	943.52664	943.52582	−0.288	MS^2[943]:925(100),927(76),486(30),859(13),927(13),845(10),827(6)	Soyasaponin I/isomer	-	+
A2	9.32	P	$C_{43}H_{71}O_{15}$	827.47875	827.47443	−3.218	MS^2[827]:709(100),809(10),691(9),768(4),737(2),695(2),577(2),335(2),467(1)	Acetylastragaloside II isomer	+	++
A3	10.43	P	$C_{38}H_{63}O_{11}$	695.43704	695.43274	−3.391	MS^2[695]:577(100),677(12),559(9),583(5),576(2)	Mongholicoside II	+	++
		N	$C_{47}H_{77}O_{19}$	945.50700	945.50916	4.023	MS^2[945]:783(100),489(3),621(2),765(1),651(1) MS^3[783]:489(100),621(53),383(35),651(26)			
A4	10.76	P	$C_{47}H_{79}O_{19}$	947.52155	947.52026	−0.788	MS^2[947]:437(100),455(52),419(42),473(22),587(21),569(16),599(12),605(11),617(7) MS^3[437]:419(100),401(18)	Agroastragaloside V	+	++
A5	11.61	N	$C_{41}H_{69}O_{14}$	785.46983	785.47198	4.834	MS^2[785]:491(100),623(26),489(15),435(6),649(6),717(4),741(1)	Cyclocanthoside E / isomer	+	++
A6*	11.79	N	$C_{41}H_{67}O_{14}$	783.45363	783.45612	4.578	MS^2[783]:489(100),621(46),651(36),383(15),453(11),515(8),471(6)	Isoastragaloside IV	++	+
A7	11.82	N	$C_{42}H_{69}O_{15}$	813.46474	813.46747	3.375	MS^2[813]:745(100),767(67),771(63),607(37),651(20),387(25)	Astramembranoside A / isomer	+	++
A8	11.89	N	$C_{41}H_{69}O_{14}$	785.46983	785.46277	−4.892	MS^2[785]:491(100),623(58),489(44),653(30),717(21),737(20)	Cyclocanthoside E / isomer	+	++
A9	12.42	N	$C_{42}H_{69}O_{15}$	813.46474	813.46729	3.154	MS^2[813]:651(100),687(64),745(47),767(44),473(26),707(23)	Astramembranoside A / isomer	+	++
		P	$C_{42}H_{71}O_{15}$	815.47930	815.47729	−1.788	MS^2[815]:437(100),455(48),419(41),473(29),599(20),653(7),278(6),437(6),467(6),745(5) MS^3[437]:419(100),351(26),175(22),215(16),253(16),167(10)			
A10	12.55	N	$C_{41}H_{69}O_{14}$	785.46983	785.47180	4.605	MS^2[785]:491(100),623(24),717(13),747(4),629(4),701(3)	Cyclocanthoside E / isomer	-	++
A11	12.59	N	$C_{43}H_{69}O_{15}$	825.46419	825.46735	3.151	MS^2[825]:765(100),783(45),757(17),787(12),779(11),673(5),401(4)	Astragaloside II isomer	+	++
A12	13.32	N	$C_{36}H_{61}O_{11}$	669.42248	669.42383	4.468	MS^2[669]:623(100),533(46),465(39),367(29),651(18)	Mongholicoside A /isomer	+	++
A13	13.79	N	$C_{43}H_{71}O_{15}$	827.48039	827.48138	3.181	MS^2[827]:759(100),767(39),784(36),357(34),781(33),616(24)785(22),770(20)	Agroastragaloside II	+	++
A14	14.00	N	$C_{43}H_{69}O_{15}$	825.46419	825.46710	4.849	MS^2[825]:633(100),763(38),765(34),645(27),486(17),643(15),783(15)	Astragaloside II isomer	-	+
A15	14.07	N	$C_{36}H_{61}O_{11}$	669.42248	669.42377	4.378	MS^2[669]:623(100),601(57),397(26),533(21),601(20),625(19),641(17),651(15)	Mongholicoside A /isomer	+	++
A16*	14.27	N	$C_{41}H_{67}O_{14}$	783.45363	783.45813	4.144	MS^2[783]:489(100),621(14),383(11),453(4)	Astragaloside IV	++	+
A17	14.55	N	$C_{41}H_{69}O_{14}$	785.46983	785.46313	−4.433	MS^2[785]:490(100),489(79),491(28),623(16),383(13),621(11)	Cyclocanthoside E / isomer	+	++
A18*	14.59	N	$C_{41}H_{67}O_{14}$	783.45363	783.45654	3.115	MS^2[783]:489(100),383(13),621(12),453(4),401(2),472(2),381(2)	Astragaloside III	++	+
A19	16.10	N	$C_{51}H_{81}O_{21}$	1029.52758	1029.52173	−4.619	MS^2[1029]:985(100),984(18),967(2)			
		P	$C_{51}H_{83}O_{21}$	1031.54214	1031.54199	−0.141	MS^2[1031]:984(100),494(57),558(52),331(50),667(49),936(48),323(47),482(46),300(45)	Agroastragaloside III	+	++
A20	16.29	N	$C_{48}H_{77}O_{18}$	941.51209	941.50549	−5.259	MS^2[941]:923(100),524(56),873(36),923(32),615(27),523(26),879(20),456(18),	Soyasaponin I/isomer	+	++
A21	16.31	N	$C_{47}H_{73}O_{17}$	909.48532	909.48804	4.192	MS^2[909]:891(100),523(50),569(49),613(49),455(35),701(31),435(18),757(16)	Acetylastragaloside I /isomer	+	++
A22*	16.67	N	$C_{43}H_{69}O_{15}$	825.46419	825.46796	3.890	MS^2[825]:765(100),633(17),621(11),461(10),489(8)	Astragaloside II	++	+

		P	$C_{43}H_{71}O_{15}$	827.47875	827.47729	−1.762	MS^2[827]:269(100),592(67),629(66),351(64),296(63),633(60),709(60),247(59),277(57)			
A23	16.74	N	$C_{36}H_{59}O_{11}$	667.40683	667.40820	4.512	MS^2[667]:649(100),449(82),621(81),299(80),450(74),485(54)	Mongholicoside B	+	++
		N	$C_{48}H_{77}O_{18}$	941.51209	941.51392	3.694	MS^2[941]:923(100),525(73),615(51),744(49),879(41),457(40),795(37),437(35),597(16)			
A24	16.85						MS^3[923]:525(100),733(55),879(47),437(44),597(28),457(21)	Soyasaponin I/isomer	+	++
		P	$C_{48}H_{79}O_{18}$	943.52664	943.52496	−1.200	MS^2[943]:599(100),797(88),441(79),423(48),617(28),581(23),520(10),269(8),454(8),867(8),448(8)			
A25	16.91	N	$C_{43}H_{69}O_{15}$	825.46419	825.46631	3.892	MS^2[825]:783(100),607(32),765(30),735(16),795(10),697(9),758(7)	Astragaloside II isomer	-	+
A26	17.53	N	$C_{42}H_{69}O_{15}$	813.46474	813.46686	4.625	MS^2[813]:767(100),274(73),677(18)	Astramembranoside A / isomer	+	++
A27*	18.12	N	$C_{43}H_{69}O_{15}$	825.46419	825.46643	4.037	MS^2[825]:765(100),633(19),717(24),495(20),351(5)	Isoastragaloside II	-	+
A28	18.80	N	$C_{42}H_{65}O_{14}$	793.43853	793.44080	4.937	MS^2[793]:631(100),725(24),657(8),724(7),747(5),718(5),697(4)	Huangqiyenin E/isomer	-	+
A29	18.83	N	$C_{42}H_{69}O_{15}$	813.46474	813.46692	4.699	MS^2[813]:767(100),677(11),795(1)	Astramembranoside A / isomer	+	++
A30	18.94	N	$C_{45}H_{71}O_{16}$	867.47476	867.47766	4.608	MS^2[867]:807(100),765(61),821(24),731(24),821(23)	Astragaloside I isomer	+	++
A31	19.16	N	$C_{47}H_{73}O_{17}$	909.48532	909.48846	4.654	MS^2[909]:891(100),455(86),569(33),523(29),613(28),407(28),763(26),773(22)	Acetylastragaloside I/isomer	+	++
A32	19.21	N	$C_{48}H_{77}O_{18}$	941.51209	941.50427	−4.555	MS^2[941]:923(100),523(44),879(37),614(36),523(36),613(32),732(31)	Soyasaponin I	+	++
A33	19.34	N	$C_{45}H_{71}O_{16}$	867.47476	867.47766	4.608	MS^2[867]:821(100),799(34),731(23),343(16),787(11)	Astragaloside I isomer	-	+
A34	19.44	P	$C_{48}H_{79}O_{18}$	943.52664	943.52161	−4.750	MS^2[943]:796(100),598(88),439(30),597(27),795(13)	Soyasaponin I/isomer	-	+
A35	20.25	N	$C_{42}H_{65}O_{14}$	793.43853	793.44073	4.849	MS^2[793]:455(100),613(86),435(85),391(45)	Huangqiyenin E/isomer	-	+
A36	20.34	N	$C_{45}H_{71}O_{16}$	867.47476	867.47662	3.410	MS^2[867]:807(100),799(52),765(51),731(44),825(43),731(29)	Astragaloside I isomer	-	+
A37*	20.95	N	$C_{45}H_{71}O_{16}$	867.47476	867.47943	4.649	MS^2[867]:781(100),807(55),821(51),765(18),747(16)	Astragaloside I	++	+
A38	22.12	N	$C_{45}H_{73}O_{16}$	869.49096	869.49335	4.644	MS^2[869]:823(100),801(46),599(18),785(15),536(11),731(10),741(8),705(8)	Agroastragaloside I	-	+
A39*	22.72	N	$C_{45}H_{71}O_{16}$	867.47476	867.47711	3.974	MS^2[867]:807(100),747(38),685(29),717(19),765(16),749(10)	Isoastragaloside I	-	+
A40	22.77	N	$C_{48}H_{73}O_{19}$	953.47570	953.47968	3.898	MS^2[953]:909(100),849(3),867(2),807(1) MS^3[909]:849(100),807(87),765(80),867(56),747(42)	Malonylastragaloside I	+	++
A41	22.87	N	$C_{47}H_{73}O_{17}$	909.48532	909.48846	4.654	MS^2[909]:849(100),867(27),765(24),801(14),807(12),747(11),867(10)	Acetylastragaloside I/isomer	+	++
A42*	23.79	N	$C_{45}H_{71}O_{16}$	867.47476	867.47754	4.470	MS^2[867]:807(100),287(75),765(73),645(65),799(63),723(34),850(31)	β-D-glucopyranoside,(3β,6α,16β,20R,24s)-3-[(3,4-di-O-acetyl-β-D-xylopyranosyl)oxy]-20,24-epoxy-16,25-dihydroxy-9,19-cyclolanostan-6-yl	-	+

Table 2. Summary of identified flavonoids in AR and FAR.

Peak	t_R /min	Ion mode	Formula	Theoretical Mass *m*/*z*	Experimental Mass *m*/*z*	Error (ppm)	MS^2/MS^3 fragment ions	Identification	FAR	AR
B1	4.37	N	$C_{29}H_{37}O_{16}$	641.20926	641.21063	4.708	MS^2[641]:479(100),317(75),595(35),611(30),623(26),379(24),610(22)	5′-hydroxy-isomucronulatol-2′,5′-di-o-glucoside	+	++
B2	4.47	P	$C_{24}H_{25}O_{12}$	505.13460	505.13318	−1.727	MS^2[505]:333(100),335(41),373(26),438(21),281(21),343(13),282(11),317(9),181(7),487(6)	Neocomplanoside/isomer	+	++
B3	4.76	N	$C_{28}H_{31}O_{16}$	623.16231	623.16388	3.165	MS^2[623]:299(100),284(31),604(7),283(6),456(6),605(5),443(5),255(4)	Complanatuside isomer	-	+
B4	5.23	N	$C_{28}H_{31}O_{16}$	623.16231	623.16364	4.780	MS^2[623]:299(100),284(32),443(10),240(4),461(3),577(2),605(2),211(2),239(2)	Complanatuside isomer	-	+
B5	5.35	N	$C_{22}H_{21}O_{11}$	461.10948	461.11050	3.773	MS^2[461]:299(100),284(9) MS^3[299]:284(100)	Kaempferol-4′-methylether-3-D-glucoside	+	++
		P	$C_{22}H_{23}O_{11}$	463.12404	463.12265	−1.809	MS^2[463]:445(100),401(4),344(4),234(3),431(1),301(1)			
B6	5.53	P	$C_{16}H_{17}O_5$	289.10760	289.10645	−2.076	MS^2[289]:271(100),270(91),221(78),205(76),233(32),261(17)	(3R)-7,2′,3′-trihydroxy-4′-methoxy isoflavonone/isomer	+	-
B7	5.99	N	$C_{16}H_{11}O_5$	283.06175	283.06198	3.642	MS^2[283]:268(100),269(3) MS^3[268]:240(100),239(49),334(46),211(44),195(23)	Calycosin isomer	-	+
		P	$C_{16}H_{13}O_5$	285.07630	285.07529	−1.614	MS^2[285]:270(100),253(44),225(18),137(7),271(5),257(3)			
B8	6.19	N	$C_{24}H_{23}O_{12}$	503.12005	503.12112	4.401	MS^2[503]:299(100),284(23),443(4),461(2),484(1),240(1)	Neocomplanoside/isomer	-	+
B9*	6.20	N	$C_{22}H_{21}O_{10}$	445.11457	445.11481	4.239	MS^2[445]:283(100),268(17)	Calycosin-7-glucoside	+	++
		P	$C_{22}H_{23}O_{10}$	447.12912	447.12695	−3.630	MS^2[447]:285(100),334(8),403(2),306(1),241(1) MS^3[285]:270(100),253(41),225(17),137(7),229(5),211(5)			
B10	6.26	P	$C_{16}H_{13}O_5$	285.07630	285.07678	3.613	MS^2[285]:270(100),253(43),225(19),137(9) MS^3[270]:137(100),253(57),214(31),242(13),134(12),213(12)	Calycosin isomer	-	+
B11	6.34	P	$C_{17}H_{15}O_6$	315.08686	315.08603	−0.903	MS^2[315]:300(100),283(20),255(8),167(5),259(4),301(2),287(2),175(2)	7,3′-dihydroxy-8,4-dimethoxyisoflavone/isomer	-	+
B12	6.22	N	$C_{22}H_{21}O_{12}$	477.10440	477.10532	4.382	MS^2[477]:315(100),301(18),300(14),347(13),313(11),458(5),278(4)	isorhamnetin-3-D-glucoside	+	++
B13	6.35	N	$C_{17}H_{13}O_6$	313.07231	313.07236	4.415	MS^2[313]:298(100),285(2),295(1),287(1),283(1)	7,3′-dihydroxy-8,4-dimethoxyisoflavone / isomer	+	++
B14	6.49	N	$C_{22}H_{21}O_9$	429.11965	429.12024	4.200	MS^2[429]:252(100),253(25),295(7),267(3),411(2),361(2),383(2),231(2)	Ononin isomer	+	-
B15	6.56	N	$C_{23}H_{23}O_{11}$	475.12513	475.12579	4.845	MS^2[475]:298(100),283(50),299(14),297(5),255(4),443(4),194(4),277(3)	Odoratin-7-O-*β*-D-glucoside/isomer	+	-
B16*	6.72	N	$C_{21}H_{19}O_{10}$	431.09727	431.09955	3.281	MS^2[431]:268(100),269(62),311(7),341(2),283(2)	Genistin	+	++
B17	6.82	N	$C_{23}H_{23}O_{11}$	475.12513	475.12619	3.687	MS^2[475]:299(100),284(13),298(7),460(5),283(2),297(2),431(1) MS^3[299]:284(100),240(1)	Odoratin-7-O-*β*-D-glucoside/isomer	+	-

		P	$C_{23}H_{25}O_{11}$	477.13969	477.13742	−3.601	MS^2[477]:301(100),345(10),199(10),183(8),453(7) MS^3[301]:286(100),269(33),153(29),245(15),241(14),152(6),223(5),175(2),273(2),123(1)		
B18	6.99	N	$C_{16}H_{11}O_5$	283.06175	283.06192	4.430	MS^2[283]:268(100),269(4) MS^3[268]:240(100),239(63),211(55),224(40),184(28),195(27)	Calycosin isomer	++	+
		P	$C_{16}H_{13}O_5$	285.07630	285.07529	−1.614	MS^2[285]:270(100),253(43),225(20),285(17),137(9),229(7),286(4),257(3),181(2)			
B19	7.02	N	$C_{16}H_{15}O_5$	287.09305	287.09225	2.961	MS^2[287]:243(100),203(53),201(19),219(11),259(9),173(7),157(5)	(3R)-7,2′,3′-trihydroxy-4′-methoxy isoflavonone/isomer	+	-
		P	$C_{16}H_{17}O_5$	289.10760	289.10651	−1.868	MS^2[289]:271(100),184(8),252(8),166(7),205(4),182(2)			
B20	7.10	N	$C_{22}H_{21}O_{10}$	445.11457	445.11575	4.351	MS^2[445]:283(100),268(17) MS^3[283]:268(100)	Calycosin-7-glucoside isomer	-	+
B21	7.16	N	$C_{17}H_{13}O_6$	313.07231	313.07230	3.224	MS^2[313]:298(100),181(17),245(8),137(6),295(6),269(5),139(5),131(3),194(3)	7,3′-dihydroxy-8,4-dimethoxyisoflavone / isomer	+	++
B22	7.25	N	$C_{21}H_{19}O_{10}$	431.09892	431.09961	3.421	MS^2[431]:268(100),269(48),311(8),413(6),341(4),323(2),412(2)	genistin isomer	-	+
B23	7.28	P	$C_{17}H_{15}O_6$	315.08686	315.08575	−1.792	MS^2[315]:300(100),283(19),255(9),269(8),297(5),167(5),259(4),138(3)	7,3′-dihydroxy-8,4-dimethoxyisoflavone / isomer	+	-
B24	7.36	N	$C_{15}H_9O_5$	269.04610	269.04352	−3.456	MS^2[269]:241(100),240(58),225(48),197(25),185(20),213(15)	5,7,4′-trihydroxy-isoflavonone / isomer	-	+
		N	$C_{16}H_{11}O_5$	283.06175	283.06189	4.324	MS^2[283]:268(100),269(1) MS^3[268]:240(100),211(58),239(55),224(40),195(25)			
B25	7.38	P	$C_{16}H_{13}O_5$	285.07630	285.07571	−0.140	MS^2[285]:270(100),253(43),225(20),285(14),137(8),229(7),286(5),257(3),181(2),197(1)	Calycosin isomer	+	++
B26*	7.52	N	$C_{28}H_{31}O_{16}$	623.16231	623.16339	4.379	MS^3[270]:137(100),253(54),214(33),213(14),134(13),242(12) MS^2[623]:461(100),299(68),443(3)	Complanaruside	-	+
B27	7.56	N	$C_{16}H_{11}O_5$	283.06175	283.06158	3.229	MS^2[283]:268(100),254(7),269(3),253(1),255(1),239(1),265(1)	Calycosin isomer	+	-
B28	7.69	P	$C_{16}H_{13}O_5$	285.07630	285.07550	−0.877	MS^2[285]:270(100),253(43),225(19),137(9),229(7),257(3),181(2) MS^3[270]:137(100),253(58),214(29),213(15),134(11),242(11)	Calycosin isomer	+	-
B29	7.70	N	$C_{24}H_{23}O_{11}$	487.12513	487.12631	3.793	MS^2[487]:283(100),268(50),427(14),193(11),419(10),253(3)	Calycosin-7-O-β-D-glucoside-6″-*o*-acetate	-	+
B30	7.80	P	$C_{17}H_{15}O_6$	315.08686	315.08594	−1.189	MS^2[315]:300(100),283(19),255(7),167(5),301(5),259(4),138(3),269(3),168(2),297(1)	7,3′-dihydroxy-8,4-dimethoxyisoflavone/isomer	+	++
		N	$C_{16}H_{11}O_4$	267.06683	267.06693	4.533	MS^2[267]:252(100),253(5),249(2)			
B31	7.87	P	$C_{16}H_{13}O_4$	269.08138	269.08215	4.886	MS^2[269]:254(100),237(51),213(35),253(13),107(9),118(6),241(6),136(5)	Formononetin isomer	+	++
B32	7.89	P	$C_{26}H_{27}O_{11}$	515.15534	515.15131	−3.751	MS^2[515]:500(100),485(76),339(75),484(56),338(31),324(30),497(27),337(19),323(18)	Calycosin-7-O-β-D-glucoside-6″-*o*-butylene ester/isomer	+	-
B33	7.93	N	$C_{29}H_{37}O_{15}$	625.21434	625.21527	4.116	MS^2[625]:301(100),463(9),286(4),445(3),607(2),271(2),473(1)	Isomucronulatol-7,2′-di-o-glucoside/isomer	+	++

B34	8.12	N	$C_{16}H_{11}O_5$	283.06175	283.06168	3.582	MS^2[283]:268(100),269(3),255(1)	Calycosin isomer	-	+
B35	8.15	N	$C_{23}H_{23}O_{11}$	475.12513	475.12598	3.245	MS^2[475]:298(100),297(48),299(30),283(23),269(12),284(10),457(10),277(6)	7,3′-dihydroxy-8,4-dimethoxyisoflavone/isomer	+	-
B36	8.24	N	$C_{16}H_{11}O_4$	267.06683	267.06702	4.870	MS^2[267]:252(100),253(1) MS^3[252]:223(100),208(65),224(54),132(21),195(15),196(5)	Formononetin isomer	+	++
B37*	8.26	P	$C_{22}H_{23}O_9$	431.13421	431.13263	−2.386	MS^2[431]:269(100),343(0.3),413(0.2)	Ononin	-	+
B38	8.41	N	$C_{17}H_{15}O_5$	299.09305	299.09293	3.115	MS^2[299]:284(100),269(1),255(1)			
		P	$C_{17}H_{17}O_5$	301.10760	301.10641	−2.126	MS^2[301]:167(100),269(26),191(21),147(19),163(12),273(11),207(9),286(6),241(6),270(3)	Pratensein/ isomer	++	+
B39	8.53	P	$C_{26}H_{27}O_{11}$	515.15534	515.15076	−4.819	MS^2[515]:339(100),321(3),199(1)	Calycosin-7-O-β-D-glucoside-6″-*O*-butylene ester	+	-
B40	8.54	N	$C_{16}H_{15}O_5$	287.09305	287.09183	1.498	MS^2[287]:272(100),135(93),165(46),177(29),121(22),147(19)	(3R)-7,2′,3′-trihydroxy-4′-methoxy isoflavonone / isomer	-	+
B41	8.70	N	$C_{29}H_{37}O_{15}$	625.21434	625.21558	−4.782	MS^2[625]:323(100),301(30),245(5),263(3),268(3),283(3),341(2),607(2)	Isomucronulatol-7,2′-di-o-glucoside/isomer	-	+
B42	8.73	N	$C_{23}H_{23}O_{11}$	475.12513	475.12601	3.308	MS^2[475]:299(100),284(62),298(18),297(17),283(9),285(9),269(9),151(1)	Odoratin-7-O-*β*-D-glucoside/isomer	+	-
B43	8.78	N	$C_{16}H_{11}O_4$	267.06683	267.06696	4.158	MS^2[267]:252(100),253(3),249(2),223(1)	Formononetin isomer	-	+
B44	8.96	N	$C_{17}H_{15}O_5$	299.09305	299.09314	3.817	MS^2[299]:284(100),269(4)			
	9.00	P	$C_{17}H_{17}O_5$	301.10760	301.10641	−2.126	MS^2[301]:167(100),269(22),191(20),147(15),163(10),273(9),207(7),241(6),286(2),270(2)	Pratensein/ isomer	+	++
B45	9.03	N	$C_{17}H_{17}O_5$	301.10870	301.10770	3.479	MS^2[301]:286(100),109(14),135(12),147(10),283(8),271(6),179(3),153(2),257(2)	(3R)-8,2′-Dihydroxy-7,4′-dimethoxy-isoflavan / isomer	++	+
	9.08	P	$C_{17}H_{19}O_5$	303.12325	303.12225	−1.485	MS^2[303]:167(100),149(32),123(19),284(16),181(14),168(7),219(6),270(5),193(5)			
B46	9.17	N	$C_{16}H_{11}O_4$	267.06683	267.06689	3.046	MS^2[267]:252(100),253(5) MS3[252]:223(100),208(70),224(46),132(16),195(15),196(7),179(3),225(2)	Formononetin isomer	+	-
		P	$C_{16}H_{13}O_4$	269.08138	269.08182	3.659	MS^2[269]:269(100),254(72),237(40),213(29),270(18),253(10),107(7),118(4),136(3) MS^3[269]:254(100),253(32),214(11),163(7)			
B47	9.23	N	$C_{17}H_{17}O_5$	301.10870	301.10880	3.811	MS^2[301]:286(100),135(19),109(15),147(10),121(8),283(6),271(6),179(6) MS^3[286]:271(100),242(8),268(5)	(3R)-8,2′-dihydroxy-7,4′-dimethoxy-isoflavan / isomer	-	+
	9.24	P	$C_{17}H_{19}O_5$	303.12325	303.12219	−1.683	MS^2[303]:167(100),149(29),123(22),181(16),193(6),285(2),219(1),168(1)			
B48*	9.25	N	$C_{23}H_{27}O_{10}$	463.16152	463.16254	3.757	MS^2[463]:301(100),299(1) MS^3[301]:286(100)	Astraisoflavan-7-O-β-D-glucoside	+	++
B49		N	$C_{17}H_{13}O_5$	297.07740	297.07748	3.823	MS^2[297]:282(100),283(4),279(3),267(2),253(2),254(1),167(1)	Afromosin	++	+

	9.40	P	$C_{17}H_{15}O_5$	299.09195	299.09119	−0.702	MS^2[299]:284(100),166(23),243(21),239(11),267(11),285(10),137(4) MS^3[284]:256(100),267(27),166(16),253(10),255(8),227(8),254(6),241(5)			
B50	9.42	N	$C_{23}H_{27}O_{10}$	463.16152	463.16241	3.477	MS^2[463]:287(100),272(3),395(3),213(1)	Astraisoflavan-7-O-β-D-glucoside isomer	+	-
B51	9.45	N	$C_{16}H_{11}O_4$	267.06683	267.06699	4.757	MS^2[267]:252(100),253(1) MS^3[252]:223(100),208(73),224(49),132(21),195(13),196(4)	Formononetin isomer	-	+
		P	$C_{16}H_{13}O_4$	269.08138	269.08035	−1.804	MS^2[269]:269(100),254(63),237(33),213(25),270(20),253(11),107(7),118(5),136(5),241(3) MS^3[269]:213(100),175(80),254(65),237(38),253(29),238(25)			
B52*	9.58	N	$C_{16}H_{11}O_5$	283.06175	283.06183	4.112	MS^2[283]:268(100),269(1) MS^3[268]:240(100),211(64),239(62),224(45),195(30),184(26)	Calycosin	++	+
		P	$C_{16}H_{13}O_5$	285.07630	285.07520	−1.929	MS^2[285]:270(100),253(43),225(20),137(9),229(7),257(3),181(2),175(1) MS^3[270]:137(100),253(50),214(35),134(13),213(13),242(10)			
B53	9.61	P	$C_{26}H_{27}O_{11}$	515.15534	515.15076	−4.819	MS^2[515]:339(100),500(7),199(7),353(1)	Calycosin-7-O-β-D-glucoside-6″-O-butylene ester/isomer	+	-
B54	9.83	N	$C_{17}H_{17}O_5$	301.10870	301.10886	4.011	MS^2[301]:286(100),109(17),135(12),147(8),271(7),283(7),259(3),121(3)	(3R)-8,2′-Dihydroxy-7,4′-dimethoxy-isoflavan / isomer	+	-
		P	$C_{17}H_{19}O_5$	303.12325	303.12247	−0.759	MS^2[303]:167(100),149(30),123(23),181(19),193(6) MS^3[267]:152(100),134(29),139(11),167(9),124(8),167(2),106(2)			
B55	9.94	P	$C_{26}H_{27}O_{11}$	515.15534	515.15472	−0.132	MS^2[515]:500(100),339(59),215(21),501(18),324(10),357(8),340(7) MS^3[500]:324(100),342(75),425(68),383(44),485(17),	Calycosin-7-O-β-D-glucoside-6″-O-butylene ester/isomer	+	-
B56	10.00	P	$C_{17}H_{15}O_6$	315.08686	315.08588	−1.379	MS^2[315]:300(100),271(49),283(21),287(13),138(12),259(11),199(9),255(7)	7,3′-dihydroxy-8,4-dimethoxyisoflavone / isomer	++	+
B57	10.04	N	$C_{17}H_{15}O_5$	299.09305	299.09329	4.319	MS^2[299]:284(100),269(4) MS^3[284]:269(100)	Pratensein/ isomer	-	+
B58	10.25	N	$C_{17}H_{15}O_5$	299.09305	299.09323	4.118	MS^2[299]:284(100),269(6),255(6),165(4),271(4)	Pratensein/ isomer	+	++
B59	10.29	N	$C_{23}H_{23}O_{11}$	475.12513	475.12598	5.245	MS^2[475]:299(100),341(5),323(4),165(3),429(2),397(2),271(2)	Odoratin-7-O--D-glucoside	+	-
		P	$C_{23}H_{25}O_{11}$	477.13969	477.13809	−2.196	MS^2[477]:301(100),401(46),199(26),269(18),458(15),405(14)			
B60	10.40	N	$C_{17}H_{17}O_5$	301.10870	301.10886	4.011	MS^2[301]:286(100),135(38),121(17),109(13),147(10),283(8),179(7),271(6) MS^3[286]:271(100),242(10),268(7),269(6)	(3R)-8,2′-dihydroxy-7,4′-dimethoxy-isoflavan/ isomer	-	+
		P	$C_{17}H_{19}O_5$	303.12325	303.12247	−0.759	MS^2[303]:167(100),149(29),123(23),181(16),193(7),285(2),261(1),167(1)			
B61	10.99	N	$C_{16}H_{11}O_4$	267.06683	267.06693	4.533	MS^2[267]:252(100),253(5),249(2)	Formononetin isomer	-	+
		P	$C_{16}H_{13}O_4$	269.08138	269.08191	3.994	MS^2[269]:254(100),237(42),213(35),66(13),253(12),107(10),118(5)			

B62	11.75	P	$C_{17}H_{17}O_5$	301.10760	301.10690	−0.499	MS^2[301]:167(100),269(22),191(20),147(16),163(10),273(10),207(7),241(6),207(4)	Pratensein/ isomer	-	+
B63*	12.20	N	$C_{16}H_{11}O_7$	315.04992	315.05081	2.796	MS^2[315]:300(100),301(3)	Isorhamnetin	++	+
B64*	13.99	N	$C_{16}H_{11}O_4$	267.06683	267.06699	4.757	MS^2[267]:252(100),253(3)	Formononetin	++	+
		P	$C_{16}H_{13}O_4$	269.08138	269.08041	−1.581	MS^2[269]:254(100),251(65),237(47),213(32),253(12),107(8)			
B65	14.79	P	$C_{17}H_{17}O_5$	301.10760	301.10666	−1.296	MS^2[301]:269(100),167(98),147(61),191(56),273(36),163(32),241(26),207(22),270(10)	Pratensein/ isomer	++	+

Note: *: Compared with the reference standards; +: detected; -: undetected; ++: more abundant.

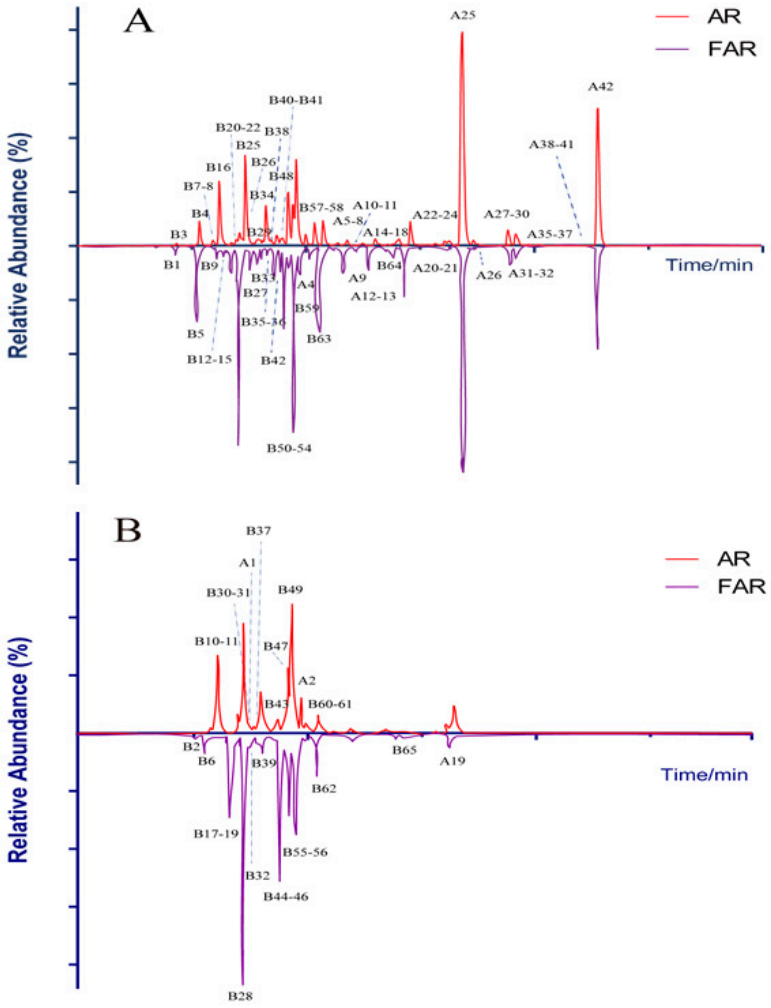

Figure 2. High-resolution extracted ion chromatograms for 107 compounds in AR and FAR. (**A**) Results of negative ion mode; (**B**) results of positive ion mode.

2.4.1. Structural Assignment of Saponins in AR and FAR

Most of the saponins in AR possess the same aglycone of cycloastragenol with different substituent groups, such as xylose, glucose, acetyl groups, and so on. They can be divided into type cyclolanostane cycloastragenol (**1–11**) or cyclolanostane cyclocanthogenin (**12–18**). Only a minority of saponins belonged to oleanane-type triterpenoids (**19**), the aglycones of which are attributed to soybean saponin B. There were 29 and 42 saponins screened and identified in FAR and AR, respectively, and their molecular formulae and chemical structures are shown in Table 3.

Table 3. Chemical information of identified saponins in AR and FAR.

No	Name	Formula	Core structure	Substituent group
1	Astragaloside I	$C_{45}H_{72}O_{16}$	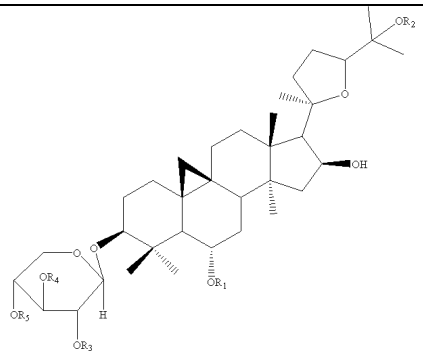	R_1=glu R_2=R_5=H R_3=R_4=Ac
2	Isoastragaloside I	$C_{45}H_{72}O_{16}$		R_1=glu R_2=R_4=H R_3=R_5=Ac
3	Astragaloside II	$C_{43}H_{70}O_{15}$		R_1=glu R_2=R_4=R_5=H R_3=Ac
4	Isoastragaloside II	$C_{43}H_{70}O_{15}$		R_1=glu R_2=R_3=R_5=H R_4=Ac
5	Astragaloside III	$C_{41}H_{68}O_{14}$		R_1=R_2=glu R_5=H R_3=R_4=Ac
6	Astragaloside IV	$C_{41}H_{68}O_{14}$		R_1=glu R_2=R_3=R_4=R_5=H
7	Isoastragaloside IV	$C_{41}H_{68}O_{14}$		R_1=R_3=R_4=R_5=H R_2=glu
8	Acetylastragaloside I	$C_{47}H_{74}O_{17}$		R_1=glu R_2=H R_3=R_4=R_5=Ac
9	Agroastragaloside III	$C_{51}H_{82}O_{21}$		R_1=R_2=glu R_5=H R_3=R_4=Ac
10	Malonylastragaloside I	$C_{48}H_{74}O_{19}$		R_1=glu R_2=H R_3=R_4=Ac R_5=malonyl
11	Astramembranoside A	$C_{42}H_{70}O_{15}$	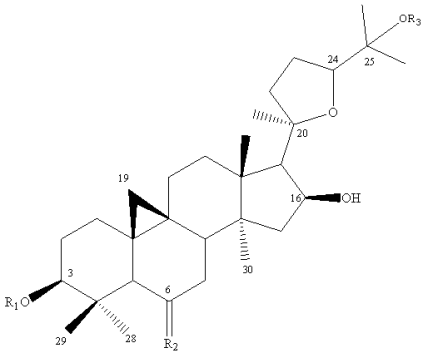	R_1=H R_2=α-O-glu β-H R_3=glu
12	MongHolicoside A	$C_{36}H_{62}O_{11}$	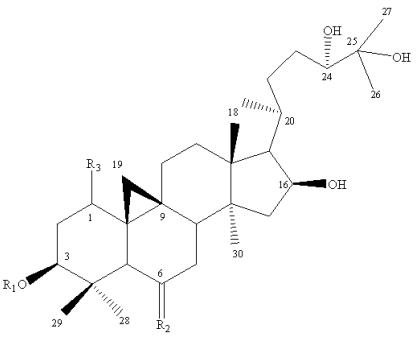	R_1=glu R_2=α-OH β-H R_3=OH
13	MongHolicoside B	$C_{36}H_{60}O_{11}$		R_1=glu R_2=O R_3=OH
14	Agroastragaloside I	$C_{45}H_{74}O_{16}$	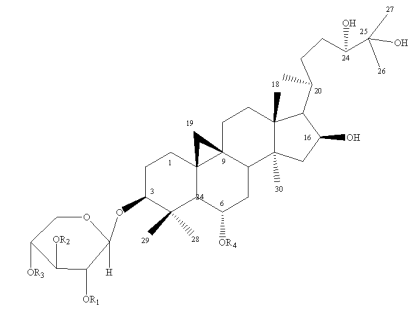	R_1=R_2=Ac R_3=H R_4=glu
15	Agroastragaloside II	$C_{43}H_{72}O_{15}$		R_1=Ac R_2=R_3=H R_4=glu
16	CyclocantHoside E	$C_{41}H_{70}O_{14}$		R_1=R_2=R_3=H R_4=glu

17	Mongholicoside II	$C_{38}H_{62}O_{11}$	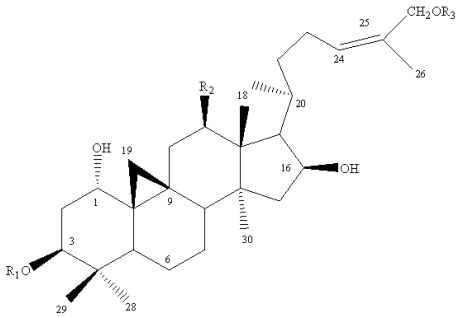	R_1= $COCH_3$ R_2=OH R_3=glu
18	Huangqiyenin E	$C_{42}H_{66}O_{14}$	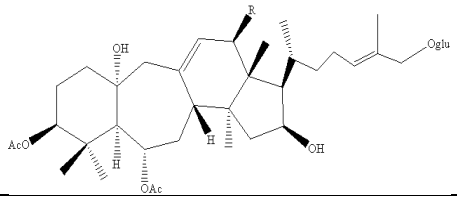	R=OAc
19	Soyasaponin I	$C_{48}H_{78}O_{18}$	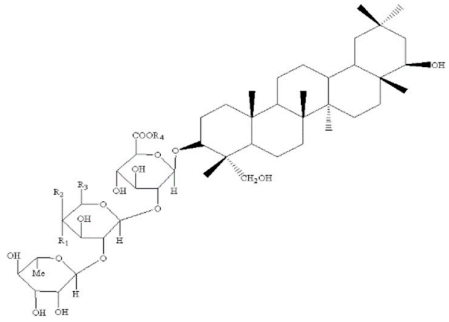	R_1=R_4=H R_2=OH R_3=CH_2OH

With retention times of 11.79 and 14.27 min, **A6** and **A16** afforded $[M-H]^-$ ions at *m*/*z* 783.45612 and 783.45813 ($C_{41}H_{67}O_{14}$, mass error within 5 ppm) in negative ion mode. Both of them produced the base peak ions at *m*/*z* 489 by neutral loss of the glucose and xylose moiety. Then, the product ion at *m*/*z* 489 further generated the predominant ion at *m*/*z* 453 by loss of $2H_2O$. Meanwhile, several important fragment ions at *m*/*z* 651 and *m*/*z* 621 were also observed due to the respective losses of xylose and glucose. Combined with standard substances, **A6** was positively characterized as isoastragaloside IV, while **A16** was speculated to be astragaloside IV.

A18 produced its $[M-H]^-$ ion at *m*/*z* 783.45654 ($C_{41}H_{67}O_{14}$) with a mass error of 3.11 ppm. In the ESI-MS^2 spectrum, further mass fragmentation resulted in *m*/*z* 489 $[M-H-Glu-Xyl]^-$, *m*/*z* 621 $[M-H-Glu]^-$, and *m*/*z* 453 $[M-H-Xyl-Glu-2H_2O]^-$, consistent with the characteristic fragmentation pathways of astragalus saponins. By comparing with the reference standard, **A18** was unambiguously identified as astragaloside III.

A2, **A11**, **A14**, **A22**, **A25**, and **A27**, which possessed a theoretical $[M-H]^-$ ion at *m*/*z* 825.46419 ($C_{43}H_{69}O_{15}$, mass error within 5 ppm), were eluted at 9.32, 12.59, 14.00, 16.67, 16.91, and 18.12 min, in order. In their ESI-MS^2 spectra, the $[M-H]^-$ ion at *m*/*z* 825 generated product ions at *m*/*z* 783, *m*/*z* 765, and *m*/*z* 633 by losing acetyl, acetyl+H_2O, and xylose moieties. Among them, **A22** was positively identified as astragaloside II, and **A27** was unambiguously characterized as isoastragaloside II based on comparison of the MS/MS spectra and retention times with reference standards. The accurate mass weight and major product ions of **A2, A11**, **A14**, and **A25** were coincident with those of **A22**, indicating that they could be astragaloside II isomers.

A30, **A33**, **A36**, **A37**, and **A39** generated an identical $[M-H]^-$ ion at *m*/*z* 867.47476 ($C_{45}H_{71}O_{16}$) with mass errors within 5 ppm. All of their deprotonated molecular ions generated a series of fragment ions at *m*/*z* 807, *m*/*z* 765, and *m*/*z* 747, corresponding to $[M-H-Ac-H_2O]^-$, $[M-H-2Ac-H_2O]^-$, and [M-H-

2Ac-2H$_2$O]$^-$. With the supplements of standard substances, **A37** was unambiguously characterized as astragaloside I, while **A39** was positively identified as isoastragaloside I. Therefore, **A30**, **A33**, and **A36** were determined to be astragaloside I isomers.

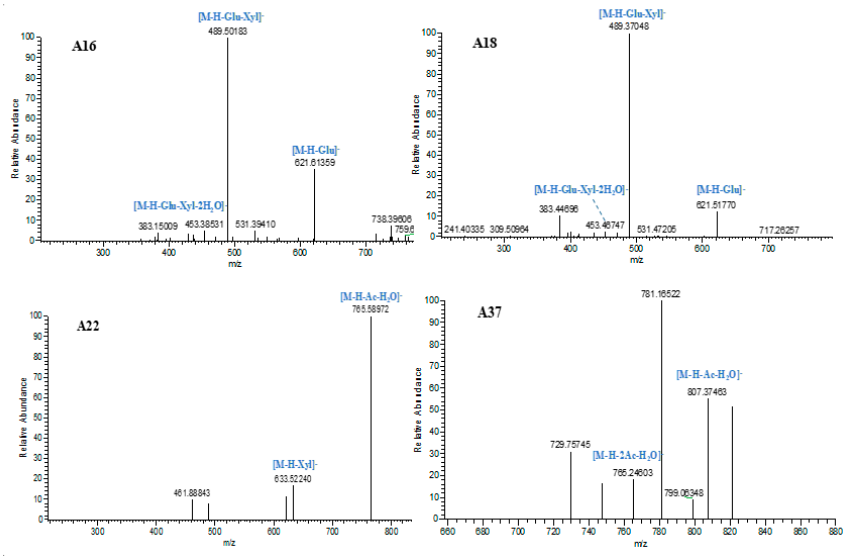

Figure 3. The ESI-MS^n spectra of A16, A18, A22, and A37.

2.4.2. Structural Assignment of Flavonoids in AR

AR contains a large number of flavonoids and glycosides, which can be divided into flavones (**1–5**), isoflavans (**6–10**), and isoflavones (**11–21**). Among these, the isoflavones are the most important group. Their molecular formulae and chemical structures are summarized in Table 4. In this work, 43 flavonoids in FAR and 47 flavonoids in AR were detected and characterized.

B9 and **B20** possessed [M-H]$^-$ ions at *m*/*z* 445.11481 and *m*/*z* 445.11575 ($C_{22}H_{21}O_{10}$, mass errors 4.23 ppm and 4.35 ppm) in negative ion mode. DPIs, including [M-H-Glu]$^-$ at *m*/*z* 283 and [M-H-Glu-CH$_3$]$^-$ at *m*/*z* 268, were also generated in their ESI-MS/MS spectra. By comparison with reference standards, **B9** was positively determined to be calycosin-7-glucoside, while **B20** was speculated to be a calycosin-7-glucoside isomer.

Two isomers, **B16** and **B22**, which displayed [M-H]$^-$ ions at *m*/*z* 431.09955 and *m*/*z* 431.09961 ($C_{21}H_{19}O_{10}$, mass error 3.28 ppm and 3.42 ppm), were eluted at 6.72 and 7.25 min, respectively. They yielded ESI-MS^2 product ions at *m*/*z* 269 [M-H-Glu]$^-$ and *m*/*z* 268 [M-2H-Glu]$^-$. **B16** was positively identified as genistin based on the comparison of the ESI-MS/MS spectra and retention time with reference standards. Meanwhile, **B22** was predicted to be a genistin isomer.

B26 was eluted at 7.52 min with an [M-H]$^-$ ion at *m*/*z* 623.16339 ($C_{28}H_{31}O_{16}$, mass error 4.379 ppm). The [M-H]$^-$ ion at *m*/*z* 623 generated characteristic fragment ions at *m*/*z* 461, *m*/*z* 443, and *m*/*z* 299. The former was generated from the neutral loss of glucose (162 Da) from the [M-H]$^-$ ion. The ion at *m*/*z* 461 was further fragmented to yield fragment ions at *m*/*z* 443 and *m*/*z* 299 by neutral loss of H$_2$O (18 Da) and glucose (162 Da). Hence, **B26** was tentatively characterized as complanaruside.

In positive ion mode, **B37** gave rise to [M+H]$^+$ ions at *m*/*z* 431.13263 with a retention time of 8.26 min. Its formula was speculated as $C_{22}H_{23}O_9$ with a mass error of −2.38 ppm. DPIs at *m*/*z* 269 [M+H-Glu]$^+$ and *m*/*z* 413 [M+H-Glu-H$_2$O]$^+$ were observed. With the addition of standard substances, **B37** was tentatively identified as ononin.

Table 4. Chemical information of identified flavonoids in AR and FAR.

No	Name	Formula	Core structure	Substituent group
1	Isorhamnetin	$C_{16}H_{12}O_7$	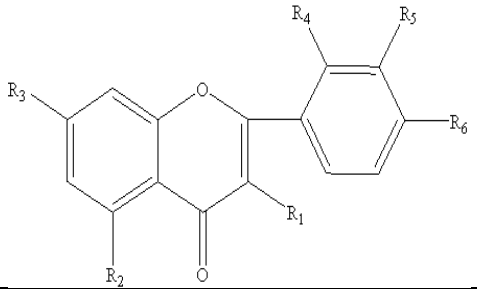	R_1=OH R_2=R_3=OH R_4=H R_5=OCH_3 R_6=OH
2	Kaempferol-4′-methylether-3-β-D-glucoside	$C_{22}H_{22}O_{11}$		R_1=O-glu R_2=R_3=OH R_4=R_5=H R_6=OCH_3
3	Isorhamnetin-3-β-D-glucoside	$C_{22}H_{22}O_{12}$		R_1=O-glu R_2=R_3=R_6=OH R_4=H R_5=OCH_3
4	Neocomplanoside	$C_{24}H_{24}O_{12}$		R_1=O-(6-O-acetyl)-glu R_4=R_5=H R_3=OCH_3 R_2=R_6=OH
5	Complanaruside	$C_{28}H_{32}O_{16}$		R_1=R_6=O-glu R_2=OH R_3=OCH_3 R_4=R_5=H
6	(3R)-7,2′,3′-trihydroxy-4′-methoxy isoflavonone	$C_{16}H_{16}O_5$	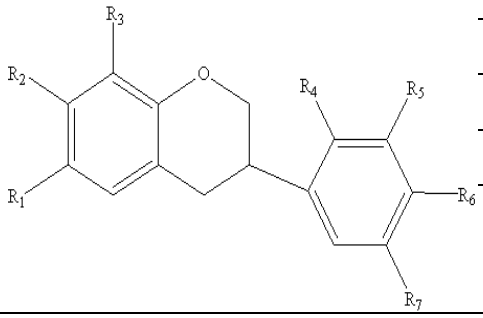	R_1=R_3=R_7=H R_2=R_4=R_5=OH R_6=OCH_3
7	(3R)-8,2′-dihydroxy-7,4′-dimethoxy-isoflavan	$C_{17}H_{18}O_5$		R_1=R_5=R_7=H R_2=R_6=OCH_3 R_3=R_4=OH
8	Astraisoflavan-7-O-β-D-glucoside isomer	$C_{23}H_{28}O_{10}$		R_1=R_3=R_7=H R_2=O-glu R_4=OH R_5=R_6=OCH_3
9	5′-hydroxy isomucronulatol 2′,5′-di-O-glucoside	$C_{29}H_{38}O_{16}$		R_1=R_3=H R_2=OH R_4=R_7=O-glu R_5=R_6=OCH_3
10	Isomucronulatol-7,2′-di-O-glucoside	$C_{29}H_{38}O_{15}$		R_1=R_3=R_7=H R_2=R_4=O-glu R_5=R_6=OCH_3
11	Formononetin	$C_{10}H_{12}O_4$	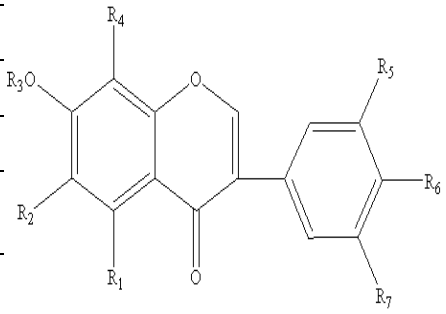	R_1=R_2=R_3=R_4=R_5=R_7=H R_6=OCH_3
12	5,7,4′-trihydroxy-isoflavonone	$C_{15}H_{10}O_5$		R_1=R_6=OH R_2=R_3=R_4=R_5=R_7=H
13	Calycosin	$C_{16}H_{12}O_5$		R_1=R_2=R_3=R_4=R_7=H R_5=OH R_6=OCH_3
14	Afromosin	$C_{17}H_{14}O_5$		R_1=R_3=R_4=R_5=R_7=H R_2=R_6=OCH_3
15	7,3′-dihydroxy-8,4′-dimethoxyisoflavone	$C_{17}H_{14}O_6$		R_1=R_2=R_3=R_7=H R_4=R_6=OCH_3 R_5=OH
16	Ononin	$C_{22}H_{22}O_9$		R_1=R_2=R_4=R_5=R_7=H R_3=glu R_6=OCH_3
17	Genistin	$C_{21}H_{20}O_{10}$		R_1=R_6=OH R_2=R_4=R_5=R_7=H R_3=glu
18	Calycosin-7-O-β-D-glucoside	$C_{22}H_{22}O_{10}$		R_1=R_2=R_4=R_7=H R_3=glu R_5=OH R_6=OCH_3
19	Calycosin-7-O-β-D-glucoside-6″-O-acetate	$C_{24}H_{24}O_{11}$		R_1=R_2=R_4=R_7=H R_3=6″-acetate-O-glu R_5=OH R_6=OCH_3
20	Calycosin-7-O-β-D-glucoside-6″-O-butylene ester	$C_{26}H_{26}O_{11}$		R_1=R_2=R_4=R_7=H R_3=6″-butylene ester-O-glu R_5=OH R_6=OCH_3
21	Odoratin-7-O-β-D-glucoside	$C_{23}H_{24}O_{11}$		R_1=R_4=R_7=H R_2=R_6=OCH_3 R_3=glu R_5=OH

In negative ion mode, **B26**, which displayed $[M-H]^-$ ions at *m*/*z* 429.11868 ($C_{22}H_{21}O_9$, mass error 1.565 ppm), was eluted at 13.38 min. In the ESI-MS^2 spectrum, it yielded product ions at *m*/*z* 411 $[M-H-H_2O]^-$ and *m*/*z* 267 $[M-H-Glc]^-$. According to the retention times of reference substances, **B26** was unambiguously identified as ononin. Besides this, **B63** was eluted at 12.20 min with $[M-H]^-$ ions at *m*/*z* 315.05081 ($C_{16}H_{11}O_7$, mass error 2.79 ppm). On account of the neutral losses of CH_2 and CH_3, DPIs at *m*/*z* 301 and *m*/*z* 300 were respectively generated in its ESI-MS^2 spectrum, which suggested the presence of a methoxy group. From the abovementioned analysis, **B63** could be deduced as isorhamnetin.

B31, **B36**, **B43**, **B46**, **B51**, **B61**, and **B64** were all observed with the same $[M-H]^-$ ions at *m*/*z* 267.06683 ($C_{16}H_{11}O_4$) with mass errors within 5 ppm. They all produced DPIs at *m*/*z* 252 $[M-H-CH_3]^-$ and *m*/*z* 253 $[M-H-CH_2]^-$ in the ESI-MS^2 spectra, corresponding to the characteristic fragmentation

pathways of a methoxy group. According to the standard references, compound **B64** was unambiguously characterized as formononetin, while the others were tentatively predicted to be formononetin isomers.

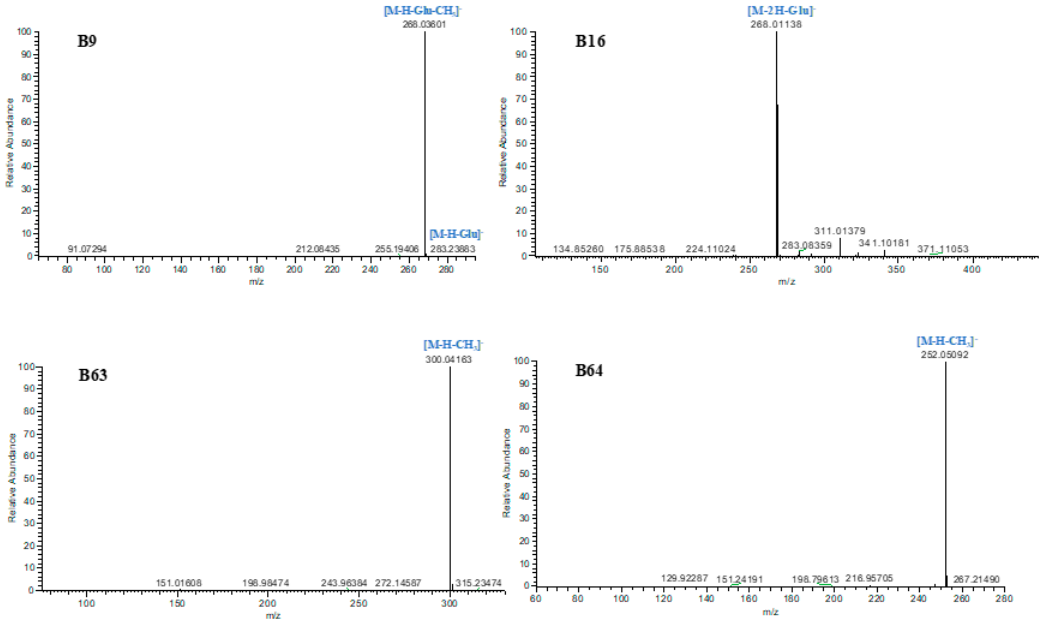

Figure 4. The ESI-MS^n spectra of B9, B16, B63, and B64.

2.4.1. Comparative Analysis of Constituents in AR and FAR

To date, more than 100 compounds have been isolated and identified from AR. Saponins and flavonoids are considered the two most important constituents of AR for displaying bioactivities in vivo or in vitro [22]. Astragaloside I, isoastragaloside I, astragaloside II, isoastragaloside II, and astragaloside IV account for more than 80% of the total saponin content. It is noteworthy that variation of the saponin content among samples of different origins and parts, even in related preparations, is remarkable [23].

In our work, we found variation of saponins and flavonoids in FAR both in quality and amount, which was different from the former AR extract. The number of saponins species in FAR decreased from 42 to 29, while quantities of certain saponins, such as isoastragaloside IV, increased with the process of fermentation. As above, the flavone aglycones reduced in number from 30 to 25. The species and quantity of flavone glycosides changed obviously, even though the number was 17 in AR as well as in FAR (shown in Figure 5).

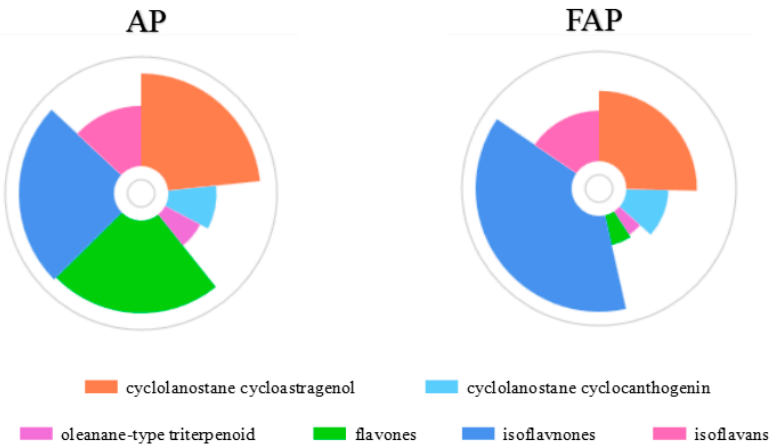

Figure 5. The classification of constituents in AR and FAR.

Moreover, the relative contents of some representative components changed greatly after fermentation (shown in Figure 6). In the process of fermentation, the contents of flavonoid glycosides—for instance, genistin, calycosin-7-glucoside, and complanaruside—dropped obviously. At the same time, the concentrations of certain saponins such as astragaloside I, astragaloside II, and isoastragaloside I decreased after fermentation, too. This result suggests that fermentation can accelerate the conversion of saponin glycosides into saponin aglycons and the hydrolysis of flavonoid glycosides to monoglycosides or aglycones. Besides this, owing to the presence of methoxyl groups, flavonoids were extremely unstable under the fermentation process. Thus, vast amounts of compounds may be altered into isomers during the fermentation process.

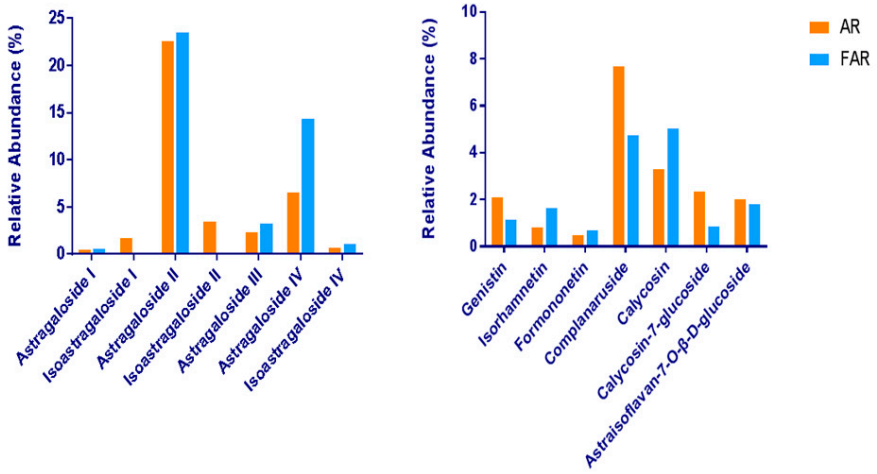

Figure 6. The changes in representative constituent contents in AR and FAR.

Noteworthily, the contents of astragaloside IV and isoastragaloside IV were significantly increased after fermentation, which means that the production of astragaloside IV was significantly higher than its consumption. It is also worth mentioning that astragaloside IV, noted for the quality control evaluation of AR in the Chinese Pharmacopeia, exhibits protective effects on cardiovascular disease, focal cerebral ischemia/reperfusion, liver cirrhosis, pulmonary disease, and diabetic nephropathy [24]. Although its content is relatively low in crude drugs, other astragalosides tend to be transformed into astragaloside IV in the fermentation process, which indicates that FAR may contribute to getting the necessary amount for the desired therapeutic effect. The probable transformations of astragaloside IV are illustrated in Figure 7.

A few issues remain with this study. For example, fermentation induced a significant difference in compounds in FAR, but no specific transforming relationship was shown. The structures of newly generated constituents in AR by fermentation of *Paecilomyces cicadae* still remain obscure, but our findings encourage a much more in-depth analysis and structural elucidation.

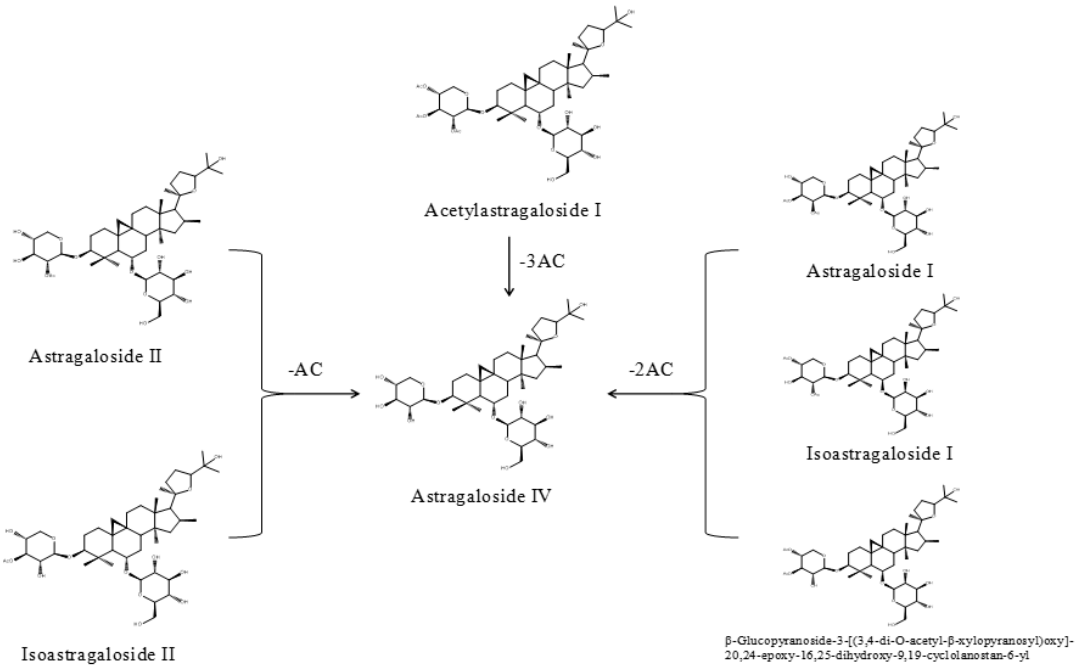

Figure 7. The probable transformations of astragaloside IV.

3. Conclusions

In the present study, an effective strategy was established for the rapid screening and identification of target constituents in AR and FAR using FS-PIL-DE acquisition coupled to DPI analysis on a hybrid LTQ-Orbitrap MS in both positive and negative ion modes. A total of 107 compounds was preliminarily identified, including 42 saponins and 65 flavonoids. Our results indicated that AR fermentation with *Paecilomyces* significantly influenced the production of saponins and flavonoids. Among these compounds, the saponins were remarkedly reduced in connection with fermentation. This may be due to the degradation of saponins or flavonoid glycosides by hydrolytic enzymes, allowing the deglycosylated main backbone of glucoside to be divided into aglycone and oligosaccharides. This is the first study to show the changes in chemical components of unfermented AR and FAR, and it provides a foundation for further studies on the chemical interaction between microbiota and AR.

4. Materials and Methods

4.1. Materials and Reagents

Astragalus membranaceus (Fisch.) Bge. var. mongholicus (Bge.) Hsiao was obtained from Beijing Bencao Fangyuan Pharmaceutical Co., Ltd. (Beijing, China) and verified by Professor Yuan Zhang (Beijing University of Chinese Medicine, China). *Paecilomyces cicadae* (Miquel*)* Samson (No. cfcc81169) was provided by China Forestry Culture Collection Center (Beijing, China). Sixteen reference compounds, including astragaloside I, astragaloside II, astragaloside III, astragaloside IV, isoastragaloside I, isoastragaloside II, isoastragaloside IV, β-D-Glucopyranoside, (3β, 6α, 16β, 20R, 24S)-3-[(3,4-di-O-acetyl-β-D-xylopyranosyl)oxy]-20,24-epoxy-16,25-dihydroxy-9,19-cyclolanostan-6-yl, calycosin, calycosin-7-glucoside, formononetin, ononin, astraisoflavan-7-Oβ-D-glucoside,

genistin, complanaruside, and isorhamnetin, were all purchased from Chengdu Must Biotechnology Co. Ltd. (Sichuan, China). Their structures were fully elucidated by comparing their spectra with the published literature. Their purities were acceptable (≥98%) according to the requirements for HPLC-UV or HPLC-ELSD analysis.

HPLC-grade acetonitrile and formic acid (FA) were purchased from Thermo Fisher Scientific (Fair Lawn, NJ, USA). All other chemicals of analytical grade were available at the work station, Beijing Chemical Works (Beijing, China). Deionized water used throughout the experiment was purified by a Milli-Q Gradient Å 10 System (Millipore, Billerica, MA, USA). Grace Pure™ SPE C_{18}-Low solid-phase extraction (SPE) cartridges (200 mg/3 mL, 59 m, 70 Å) were purchased from Grace Davison Discovery Science (Deerfield, IL, USA).

4.2. Fermentation of AR

AR was hot-air-dried for 2 days and then ground into a powder through a 100-mesh screen form using a blender. Laboratory-scale fermentation using AR was carried out in a 500 mL shake flask with a 250 mL working volume including 50 g of AR powder. A quantity of 50 g of AR powder was dissolved with 250 mL of distilled water and extracted at 121 °C for 15 min by autoclaving. *Paecilomyces cicadae* (Miquel) Samson grown at 5% (v/v) in PDA liquid medium was used as an inoculum. The mixture was fermented at 28 °C for 7 days on a rotatory shaker at 120 rpm·min^{-1}. Samples were taken on the 14th day of fermentation for analyses. Unfermented AR was ground into a powder using a 100-mesh screen, inoculated into distilled water without *Paecilomyces cicadae* (Miquel) Samson, and cultured for 7 days at 28 °C under aerobic conditions.

A volume of 1 mL of AR and FAR solution was added into an SPE cartridge pretreated with 5 mL methanol and 5 mL deionized water, in that order. Afterwards, the SPE cartridges were successively washed with 3 mL deionized water and 3 mL methanol, separately. The methanol eluate was evaporated to dryness by water bath at 70 °C. Then, the residue was re-dissolved in 200 μL methanol solution and centrifuged for 30 min (13,500 rpm, 4 °C). The supernatant was used for subsequent analysis.

4.3. UHPLC-LTQ-Orbitrap MS Analysis

4.3.1. Instrument and Conditions

UHPLC analysis was performed on a DIONEX Ultimate 3000 UHPLC system (Thermo Fisher Scientific, Waltham, MA, USA), equipped with a binary pump, an auto-sampler, a column compartment, and an electrospray ionization source. The chromatographic separation was carried out at 40 °C using a Waters ACQUITY HSS T3 column (2.1 × 100 mm i.d., 1.8 μm; Waters Corporation, Milford, MA, USA). The mobile phase consisted of 0.1% FA aqueous solution (A) and acetonitrile (B) at a flow rate of 0.3 mL/min, and the linear gradient procedure was as follows: 0–6 min, 8%–30% B; 6–14 min, 30%–40% B; 14–20.5 min, 40%–50% B; 20.5–26 min, 30%–40% B; 26–30 min, 40%–95% B. The injection volume was 2 μL.

HRMS and MS/MS spectra were obtained using LTQ-Orbitrap MS with optimized operating parameters set as follows. Positive ion mode: sheath gas (nitrogen) flow rate of 40 arb, auxiliary gas (nitrogen) flow rate of 20 arb, capillary temperature of 350 °C, spray voltage of 4.0 kV, capillary voltage of 25 V, tube lens voltage of 110 V. Negative ion mode: sheath gas (nitrogen) flow rate of 40 arb, auxiliary gas (nitrogen) flow rate of 20 arb, capillary temperature of 350 °C, spray voltage of 3.0 kV, capillary voltage of −35 V, tube lens voltage of −110 V. The metabolites were detected by full-scan mass analysis from *m*/*z* 100 to *m*/*z* 1200 with a resolution of 30,000 in positive and negative ion modes. The collision energy for collision induced dissociation (CID) was adjusted to 40% of the maximum. Dynamic exclusion (DE) was used to prevent duplication. The repeat count was set to 5, and the dynamic repeat time was 30 s with a dynamic exclusion duration of 60 s. In addition, MS^n stages of the obtained datasets were employed using the PIL-DE dependent acquisition mode.

4.3.2. Data Processing

A Thermo Xcalibur 2.1 (Thermo Scientific) workstation was used for data acquisition and data processing. In order to acquire as many fragment ions as possible, we selected the peaks with intensity over 10,000 for negative ion mode and over 40,000 for positive ion mode to identify components in AR and FAR. Based on the accurate mass, potential element compositions, and occurrence of possible reactions, the predicted atoms for chemical formulae of all the deprotonated and protonated molecular ions were set as follows: C [0–50], H [0–90], O [0–30], and ring double bond (RDB) equivalent value [0–15]. The maximum mass errors between the measured and calculated values were fixed within 5 ppm. All the relevant data, including peak number, retention time, accurate mass, the predicted chemical formula, and corresponding mass error, were recorded.

Supplementary Materials: Figure S1: Proposed fragmentation pathways for representative flavonoids detected in negative ion mode; Figure S2: Proposed fragmentation pathways for representative saponin detected in negative ion mode

Author Contributions: J.Z. conceived and designed the experiments; L.D. supervised the experimental plan; X.M., W.S., Z.G. and Z.L. performed the experiments; Y.W., X.Z. and J.L. analyzed the data; Y.W. wrote the paper; J.Z. and L.D. reviewed the manuscript; all authors read and approved the final manuscript.

Funding: This work was financially supported by the Beijing Nova Program (Z171100001117029) and the Beijing University of Chinese Medicine Fund for Distinguished Young Scholars (No. 2018-JYB-XJ008).

Conflicts of Interest: The authors declare no conflict of interest.

References

1. Xu, L.; Du, B.; Xu, B.J.F.C. A systematic, comparative study on the beneficial health components and antioxidant activities of commercially fermented soy products marketed in China. *J. Food Chem.* **2015**, *174*, 202–213.
2. Stanton, C.; Ross, R.P.; Fitzgerald, G.F.; Sinderen, D.V. Fermented functional foods based on probiotics and their biogenic metabolites. *J. Curr. Opin. Biotechnol.* **2005**, *16*, 198–203.
3. Yang, H.J.F.S. Study on Submerged Fermentation of Ganoderma lucidum into Chinese Pharmaceatical Edible Prodct. *J. Food Chem.* **2003**, *24*, 99–102.
4. Hussain, A.; Bose, S.; Wang, J.H.; Yadav, M.K.; Mahajan, G.B.; Kim, H. Fermentation, a feasible strategy for enhancing bioactivity of herbal medicines. *J. Food Res. Int.* **2016**, *81*, 1–16.
5. Wang, Y.; He, P.; He, L.; Huang, Q.; Cheng, J.; Li, W.; Liu, Y.; Wei, C. Structural elucidation, antioxidant and immunomodulatory activities of a novel heteropolysaccharide from cultured Paecilomyces cicadae (Miquel.) Samson. *J. Carbohydr. Polym.* **2019**, *216*, 270–281.
6. Ke, B.J.; Lee, C.L. Cordyceps cicadae NTTU 868 mycelium prevents CCl 4 -induced hepatic fibrosis in BALB/c mice via inhibiting the expression of pro-inflammatory and pro-fibrotic cytokines. *J. Funct. Foods* **2018**, *43*, 214–223.
7. Wang, J.; Nie, S.; Cui, S.W.; Wang, Z.; Phillips, A.O.; Phillips, G.O.; Li, Y.; Xie, M. Structural characterization and immunostimulatory activity of a glucan from natural Cordyceps sinensis. *J. Food Hydrocoll.* **2017**, *67*, 139–147.
8. Fu, J.; Wang, Z.; Huang, L.; Zheng, S.; Wang, D.; Chen, S.; Zhang, H.; Yang, S. Review of the botanical characteristics, phytochemistry, and pharmacology of Astragalus membranaceus (Huangqi). *J. Phytother. Res.* **2015**, *28*, 1275–1283.
9. Cho, W.C.; Leung, K.N. In vitro and in vivo anti-tumor effects of Astragalus membranaceus. *J. Cancer Lett.* **2007**, *252*, 43–54.
10. Liu, P.; Haiping, Z.; Yumin, L. Anti-Aging Implications of Astragalus Membranaceus (Huangqi): A Well-Known Chinese Tonic. *J. Aging Dis.* **2017**, *8*, 868.
11. Lv, Y.W.; Hu, W.; Wang, Y.L.; Huang, L.F.; He, Y.B.; Xie, X.Z. Identification and determination of flavonoids in astragali radix by high performance liquid chromatography coupled with DAD and ESI-MS detection. *J. Mol.* **2011**, *16*, 2293.
12. Lyu, M.; Wang, Y.F.; Fan, G.W.; Wang, X.Y.; Xu, S.Y.; Zhu, Y. Balancing Herbal Medicine and Functional Food for Prevention and Treatment of Cardiometabolic Diseases through Modulating Gut Microbiota. *J. Front. Microbiol* **2017**, *8*, 2146.

13. Li, S.; Wu, D.; Lv, G.; Zhao, J. Carbohydrates analysis in herbal glycomics. *J. Trends Anal. Chem.* **2013**, *52*, 155–169.
14. Kim, B.G.; Shin, K.S.; Yoon, T.J.; Yu, K.W.; Ra, K.S.; Kim, J.M.; Kim, S.Y.; Suh, H.J. Fermentation of Korean Red Ginseng byLactobacillus plantarumM-2 and Its Immunological Activities. *J. Appl. Biochem. Biotechnol.* **2011**, *165*, 1107–1119.
15. Zhang, J.Y.; Wang, Z.J.; Zhang, Q.; Wang, F.; Ma, Q.; Lin, Z.Z.; Lu, J.Q.; Qiao, Y.J. Rapid screening and identification of target constituents using full scan-parent ions list-dynamic exclusion acquisition coupled to diagnostic product ions analysis on a hybrid LTQ-Orbitrap mass spectrometer. *J. Talanta* **2014**, *124*, 111–122.
16. Zhang, J.Y.; Wang, Z.J.; Li, Y.; Liu, Y.; Cai, W.; Li, C.; Lu, J.Q.; Qiao, Y.J. A strategy for comprehensive identification of sequential constituents using ultra–High–performance liquid chromatography coupled with linear ion trap–Orbitrap mass spectrometer, application study on chlorogenic acids in Flos Lonicerae Japonicae. *J. Talanta* **2016**, *147*, 16–27.
17. Shang, Z.; Cai, W.; Cao, Y.; Wang, F.; Wang, Z.; Lu, J.; Zhang, J. An integrated strategy for rapid discovery and identification of the sequential piperine metabolites in rats using ultra high-performance liquid chromatography/high resolution mass spectrometery. *J. Pharm. Biomed. Anal.* **2017**, *146*, 387.
18. Liang, Y.; Zhao, W.; Wang, C.; Wang, Z.; Wang, Z.B.; Zhang, J.Y. A Comprehensive Screening and Identification of Genistin Metabolites in Rats Based on Multiple Metabolite Templates Combined with UHPLC-HRMS Analysis. *J. Mol.* **2018**, *23*, 1862.
19. Zhang, J.; Wang, F.; Cai, W.; Zhang, Q.; Liu, Y.; Li, Y.; Liu, R.; Cao, G. Identification of metabolites of gardenin A in rats by combination of high-performance liquid chromatography with linear ion trap-Orbitrap mass spectrometer based on multiple data processing techniques. *J. Biomed. Chromatogr.* **2015**, *29*, 379–387.
20. Wang, S. Fragment ion diagnostic strategies for the comprehensive identification of chemical profile of Gui-Zhi-Tang by integrating high-resolution MS, multiple-stage MS and UV information. *J. Pharm. Biomed. Anal.* **2014**, *98*, 22–35.
21. Zhao, W.; Shang, Z.; Li, Q.; Huang, M.; He, W.; Wang, Z.; Zhang, J. Rapid Screening and Identification of Daidzein Metabolites in Rats Based on UHPLC-LTQ-Orbitrap Mass Spectrometry Coupled with Data-Mining Technologies. *J. Mol.* **2018**, *23*, 151.
22. Chu, C.; Qi, L.W.; Li, B.; Gao, W.; Li, P. Radix Astragali (Astragalus): Latest Advancements and Trends in Chemistry, Analysis, Pharmacology and Pharmacokinetics. *J. Curr. Org. Chem.* **2010**, *14*, doi:10.2174/138527210792927663.
23. Yu, Q.T.; Qi, L.W.; Li, P.; Yi, L.; Zhao, J.; Bi, Z. Determination of seventeen main flavonoids and saponins in the medicinal plant Huang-qi (Radix astragali) by HPLC-DAD-ELSD. *J. Sep. Sci.* **2015**, *30*, 1292–1299.
24. Liu, Z.H.; Liu, H.B.; Wang, J. Astragaloside IV protects against the pathological cardiac hypertrophy in mice. *J Biomed. Pharmacother.* **2018**, *97*, 1468–1478.